Electrochimica Acta 151 (2015) 517–524

Contents lists available at ScienceDirect

Electrochimica Acta

journal homepage: www.elsevier.com/locate/electacta

Single precursor route to efficient cobalt sulphide counter electrodes for dye sensitized solar cells

M. Congiu [a,*], L.G.S. Albano [a], F. Decker [a,c], C.F.O. Graeff [a,b]

[a] UNESP–Univ. Estadual Paulista, POSMAT-Programa de Pós-Graduação em Ciência e Tecnologia de Materiais, Av. Eng. Luiz Edmundo Carrijo Coube 14-01, Bauru, SP 17033-360, Brazil
[b] DC-FC-UNESP–Univ. Estadual Paulista, Av. Eng. Luiz Edmundo Carrijo Coube 14-01, Bauru, SP 17033-360, Brazil
[c] University of Rome "La Sapienza", Department of Chemistry, Piazzale Aldo Moro 5, Rome, RM, Italy

ARTICLE INFO

Article history:
Received 28 August 2014
Received in revised form 26 October 2014
Accepted 1 November 2014
Available online 7 November 2014

ABSTRACT

In this work a novel preparation method is proposed for the one step synthesis and thin-film deposition of cost effective counter electrodes for dye sensitized solar cells (DSSC). This method is fast and allows depositing CoS nanoparticles onto F-doped SnO2 (FTO) substrates within 2 hours. The cost of reagents needed is significantly less than the cost of the products based on hexachloroplatinic acid used in the production of platinum transparent counter electrodes, and the method is compatible with the ink-jet and screen-printing technologies. The whole process does not require expensive equipment and is of simple implementation. Electrochemical Impedance Spectroscopy, Cyclic Voltammetry and I-V curves under simulated sunlight were used to characterize the electrode efficiency and stability. The counter electrodes prepared according to our procedure were transparent and show good catalytic activity with the I-/I_3- redox couple in a high stability electrolyte for DSSC (HSE). Under the best deposition conditions the charge transfer resistance of the electrodes was 1.3 Ωcm^2, less than that of the screen printed platinum on FTO glass (2.3 Ωcm^2). Power conversion efficiencies up to 6.6% were reached using the CoS counter electrodes. The optimized CoS counter electrodes were demonstrated to work also with a ferrocene besed redox liquid electolyte.

1. Introduction

The technology of dye-sensitized solar cell (DSSC) [1] is very promising for solar energy conversion due to its relatively low production costs and high power conversion efficiency attained so far, up to 13% [2]. Perhaps the most interesting characteristic of DSSC is the relatively simple technology needed to produce cells at the prototype scale, in comparison with the technology used for the production of silicon-based, or of other solid-state semiconductor-based solar cells. In fact several industrial techniques such as screen-printing (SP) and doctor blade are commonly used in the production of large-area DSSC. Basically a DSSC is composed by 5 elements: a transparent conductive oxide layer (TCO), a dye, a mesoporous TiO_2 film, an I^-/I_3^- based electrolyte and a catalytically active cathode. In order to obtain a solar cell with a good solar efficiency, the starting components above need to be properly assembled by means of an appropriate procedure for dying the mesoporous TiO_2 film, a wise choice of the spacer between the Working Electrode (WE) and the Counter-Electrode (CE), an accurate cell filling technique and a careful sealing of the device. The quality of the materials and the performance of each single component contribute to the overall efficiency of the solar cell. The CE is crucial for the correct functioning of the solar cell, since it is responsible for the electrochemical reduction reaction of I_3^- to three I^-, and consequently for the overall cell series resistance which stems in part from the charge-transfer resistance at each electrode. Generally, the counter electrode consists of a thin film of platinum nanoparticles, which are deposited on TCO by sputtering or screen printing [3,4]. Platinum is a rare and expensive material and its use affects the overall cost of the device. The search for alternative materials to platinum is important to lower the production costs of DSSC. In a recent review article Sining Yun et al. [5], highlighted the importance of the printing and *In-Situ* growth processes as directions for the future researche on Pt-free counter electrodes. In recent years several alternative materials for DSSCs counter electrodes such as graphene [6], carbon nanotubes [7], metallic PEDOT [8] and transition metal sulfides [9] have been proposed for the substitution of Pt. The class of alternative materials more promising is the metal sulfides, due to its relatively low cost, durability and easy processing. In this class of materials

* Corresponding author. Tel.: +55 14 3103 6084x7662/981402118.
E-mail address: mirko.congiu@fc.unesp.br (M. Congiu).

http://dx.doi.org/10.1016/j.electacta.2014.11.001
0013-4686/

cobalt sulfides (Co_xS_y) have shown very high catalytic activity, comparable to Pt, for I_3^-/I^- electrolyte. In 2009 a flexible CoS counter electrode was obtained by electro-deposition (ED) on ITO/PEN substrates, with 6.5% conversion efficiency [10]. In a recent work Jie Yang et al., reached conversion efficiencies of 6.81% and 6.59% using Co_3S_4 deposited on FTO by a solvothermal process (ST) [11]. Another highly efficient CoS-based counter electrode has been proposed by Srinivasa Rao et al. [12] growing CoS_2 on FTO by chemical bath deposition (CBD). A weak point of ED and CBD for the production of Co_xS_y counter electrodes, is that in both techniques electrochemical baths with high purity reagents and toxic precursors such as thiourea are necessary. Furthermore, such techniques are not commonly used for DSSC production in large scale, which is usually performed by screen-printing techniques. Indeed either counter and photo electrode were so far mostly prepared by screen-printing, using commercial TiO_2 or Pt pastes. In the case of Pt pastes and inks, a chemical precursor (hexachloroplatinic acid) is used instead of the metal nanoparticles since it gives a thin discontinuous layer of Pt nanoparticles instead of a thick metal film. On the other hand, the use of nanoparticles suspensions in pastes is more appropriated for the production of a thick mesoporous films, as in the case of TiO_2 photo anodes (4 – 8 μm thick) [13,14]. Another advantage of using a precursor solution instead of nanoparticles suspension is the lack of aggregation and precipitation that influences the long-term stability of the device. Several chemical precursors, normally organic complexes of transition metals, can be thermally converted to metal sulfides. For example in 2010 Jen-La Plante et al. published a single precursor route for the growth of nanostructures of CuS, PbS, ZnS and Ni_2S_3 by thermal decomposition of different diethyldithiocarbamates [15]. In another work, Larsen et al. proposed a solvent-less synthesis of Cu_2S nanorods from thiolate precursors.

Within this work we propose a novel and simple route to the deposition of CoS for large-scale production of counter electrodes for DSSC. The method uses cobalt(II) bis diethyl dithiocarbamate ($Co(DTC)_2$) as precursor and a thermal treatment compatible with the annealing procedures used so far for the production of mesoporous oxide WE.

2. Materials and methods

All solvents and reagents used in this work were purchased from Sigma-Aldrich, Brazil. The aqueous solutions were prepared using deionized water (Milli-q Millipore, R > 18.0 MΩ). The transparent TiO_2 paste, platinized FTO glass slides and high stability electrolyte (HSE) BV12 were purchased from DYERS S.R.L. (Rome, Italy). Electrochemical Impedance Spectroscopy (EIS) and current versus potential analysis (IxV) were performed using a Metrohm Autolab PGStat 330. A Newport full spectrum solar simulator with a 150 W lamp and AM1.5 filter was used for illumination. Powder XRD patterns were collected with a diffractometer DMAX Ultima (Rigaku International Corporation, Tokyo, Japan) using CuK_{a1} radiation, operating at 40 kV and 20 mA. Scans were performed from 5 ° to 80 ° with a step size of 0.02 ° with a scan speed of 2°/min. Scanning electron microscopy was performed using a SEM-FEG, JEOL 7500 F. Thermogravimetry (TG) and Differential Scan Calorimetry (DSC) were performed on a Netzsch Thermische Analyse - STA 409 equipment, in nitrogen atmosphere.

2.1. Synthesis of the chemical precursor

Cobalt (II) bis-diethyl dithiocarbamate ($Co(DTC)_2$) was prepared using the method described by Jen-La Plante et al. [15] for the preparation of copper diethyl dithiocarbammate. Briefly, a freshly prepared solution of sodium diethyl dithiocarbamate trihydrate (NaDTC) 1 M was slowly dropped into a solution of cobalt(II) chloride 0.5 M under continuous stirring. The precipitate was filtered and washed several times with cold isopropanol and water and then dried at room temperature.

2.2. Preparation of the counter electrodes

The precursor solutions were prepared dissolving $Co(DTC)_2$ in chloroform with 50, 25, 12.5 and 2.5 mM concentration. The precursor solution was kept in the refrigerator (4 °C) and protected from light. Before deposition, the substrates (glass or FTO on glass) were cleaned in an ultrasound bath using water, acetone and isopropanol. The precursor solution was dropped on the substrates (50 μL cm^{-1}) and the solvent was slowly evaporated under an inverted funnel. The CEs were thermally treated in an evacuated quartz tube oven (at 10^{-2} Torr) following a two-step heating program. In the first step the temperature was increased to 300 °C for 30 min with a rate of 10 °C min^{-1}. Then the temperature was increased to 400 °C with a rate of 15 °C min^{-1} and kept at 400 °C for 30, 60 and 120 min. The electrodes were slowly cooled to ambient temperature. To avoid oxidation the thermal treatment of all samples was performed under vacuum, after flushing several times the reaction chamber with high purity nitrogen (H_2O, O_2< 5 ppm). The electrodes were rinsed in acetone and then in isopropanol and kept dry until use. These electrodes were stable along time, see the Discussion section.

2.3. Symmetric cells and DSSCs assembly

Two CoS CEs were sealed facing each other using a hot-melt Bynel® (DuPont) spacer, the active area of each electrode being 0.5 cm^2. Commercial HSE electrolyte was injected in the cell by vacuum back filling then sealed with a thermoplastic.

The photo electrodes were prepared using TiO_2 paste and screen-printing technique on FTO-glass substrates with 0.25 cm^2 (N719 dye) or 1 cm^2 (N3 dye) of active area. The TiO_2 films were synthesized at 480 °C for 60 min. After cooling down to 80 °C the electrodes were sensitized by immersion in an ethanol N3 or N719 dye solution (0.3 mM) for 12 h at room temperature. After colouration, the electrodes were cleaned with ethanol and dried in nitrogen flux. The sensitized photo electrode and counter electrode were sandwiched and sealed with Bynel and the electrolyte was injected by vacuum back-filling.

2.4. Characterization

X-ray diffraction spectra were registered on powder samples. The powders were prepared using $Co(DTC)_2$ (50–100 mg) treated under the same conditions as the films. The crystallographic phase was determined matching the spectra with the Joint Committee on Powder Diffraction Standards library. The average size of the crystals was calculated from Scherrer's equation. EIS measurements were performed, on symmetric devices and complete DSSCs, from 100 MHz to 100mHz at 0 V, single sine wave (±10 mV). The measurements were performed at 25 °C. Cyclic voltammetry curves were registered at different scan rates 10, 30 and 50 mVs^{-1}. The stability of the electrodes was evaluated exposing the symmetric devices to several I-V cycles at 10mVs^{-1}; EIS spectra were taken after each treatment. The photovoltaic parameters were calculated from J-V curves under 1 sun (AM 1.5 illumination). For each batch of DSSCs, two cells were assembled using the screen-printed platinum counter electrodes. In order to evaluate the transparency of the counter electrodes, transmittance spectra of the electrodes were registered immediately after the cleaning process and confronted with that of the platinised CEs. The

wavelength for the transmittance analysis was varied between 400 and 700 nm. In order to evaluate the stability, the electrodes were subjected to typically 200 slow (10 mV/s) voltammetry scan cycles from -1.0 V to 1.0 V. Every 25 complete scans, an EIS spectrum was registered in order to calculate R_s, R_{ct} and the capacitance of the double layer.

3. Results

The thermal degradation of $Co(DTC)_2$ was studied using TG and DSC and the resulting curves are plotted in Fig 1. In the low T part of the TG curve, between 25 °C and 130 °C there is a slight mass change due to the loss of water (humidity).

An endothermic peak at 255 °C can be seen in Fig. 1, that corresponds to the precursor's melting point. The degradation of the complex starts at 267 °C and is completely converted into CoS between 350 °C and 400 °C. No significant mass changes are seen at higher temperatures. So the process temperature was fixed at 400 °C in order to ensure the complete degradation of the chemical precursor.

X-ray powder diffraction shown in Fig. 2 confirmed the crystal structure of CoS to be hexagonal (JCPDS: 03-065-3418). Notice that no other crystal phases besides hexagonal CoS is observed. As shown in Fig. 2 the XRD patterns changes with the annealing time. Each peak was fitted with a Gaussian function in order to calculate the average crystal size from Scherrer equation. The average crystal sizes for annealing times of 120, 60 and 30 minutes were 90 nm, 61 nm and 35 nm, respectively.

A typical SEM image of a CoS counter electrode is presented in Fig. 3a. As can be seen, the films consists of a uniform layer of CoS nanoparticles. From the Fig. 3b we can see, with an higher magnification, that the diameter of the nanoparticles is compatible with the average crystal size calculated through the XRD peacks. Energy-dispersive X-Ray spectroscopy (EDX) was performed on several regions showing that the films are composed of only CoS, and that the precursors have been completely reacted. More details about the EDX are provided in the supporting material. The films have a good adhesion to the FTO-glass substrate.

In order to evaluate the catalytic efficiency of the counter electrode, the charge transfer resistance (R_{ct}) was measured by EIS and compared to screen-printed Pt for different precursor concentrations. The results of the fitting are presented in Table 1. The impedance spectra plotted in Fig. 4 show that the R_{ct} of the cobalt counter electrodes is comparable to that of commercial platinum electrodes. The best results were obtained using the

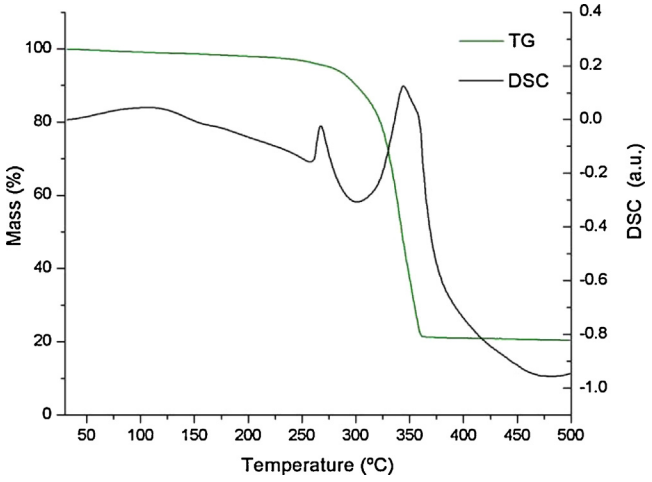

Fig. 1. Thermal decomposition analysis of $Co(DTC)_2$ from 50 to 500 °C. Thermogravimetry (green) and differential scanning calorimetry (black).

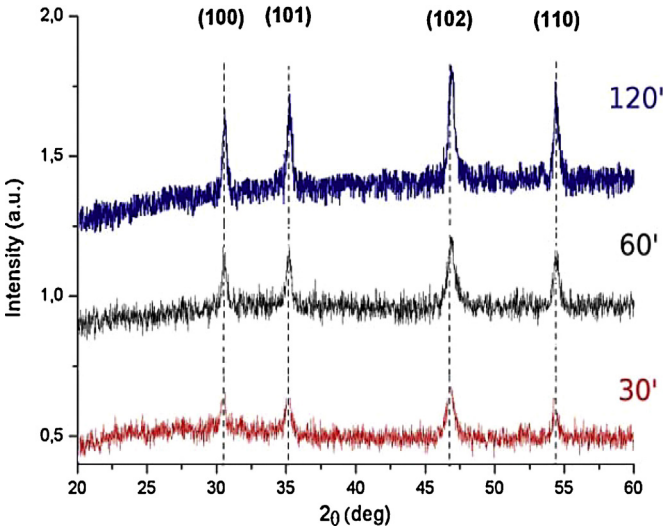

Fig. 2. Powder X-Ray diffractogram after thermal treatment at different processing times: 120, 60, and 30 min(′).

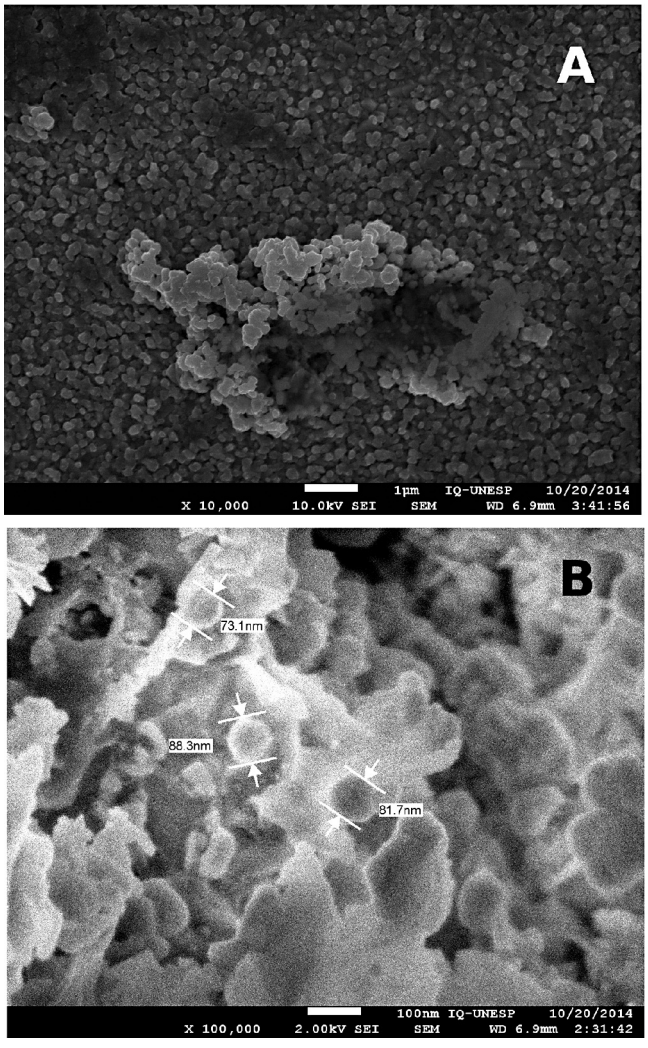

Fig. 3. A) Secondary electron (SEI) image of scanning electron microscopy (SEM) of the CoS(25) counter electrode after the deposition on FTO substrates with 10.00 kV and 10.00 X. B) Higher magnification (100.000X) of the region, in the image it is possible to see the nanoparticles.

Table 1
Table of equivalent circuit fitted EIS parameter of the electrodes in dummy cell and DSSC; series resistance (R_s), charge transfer resistance (R_{ct}), double layer capacitance (CPE Q), the exponent n.*The concentration of the precursor solution in parenthesis are in mM.** The dummy cell was filled with the ferrocene-based liquid electrolyte. ***The measurement was performed on a DSSC device and the data were calculated at V_{oc} in the dark.

Electrode (C)*	Annealing time (min)	Rs (Ω cm^2)	Rct (Ω cm^2)	CPE Q (μF cm^{-2})	n
Platinum	15	9.21	2.32	40.9	0.998
CoS(50)	120	9.84	1.91	23.7	0.996
CoS(25)	120	6.72	1.31	24.7	0.996
CoS(25)	60	7.22	1.34	29.1	0.941
CoS(25)	30	8.57	1.33	28.1	0.871
CoS(25) Fc**	120	11.10	2.27	18.0	0.848
DSSC CoS(25)***	120	4.85	1.26	30.1	0.898
CoS(12.5)	120	9.61	8.70	28.0	0.997
CoS(2.5)	120	7.30	24.21	26.9	0.995

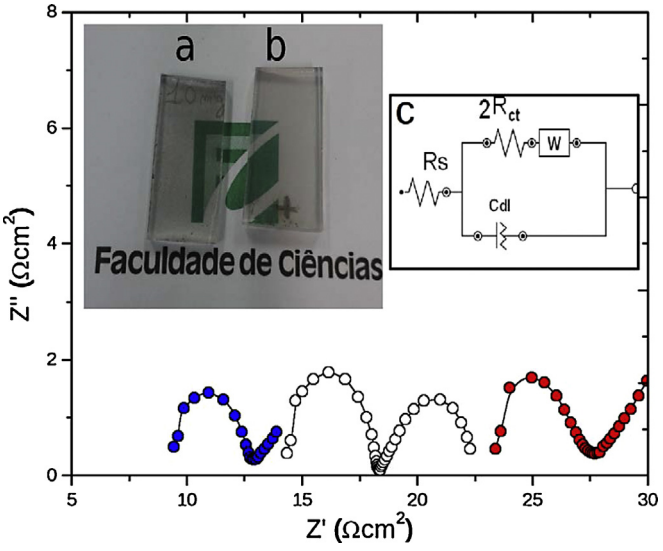

Fig. 4. Nyquist plots of the electrodes in dummy cells. The plotted semicircles are referred to: screen printed Platinum (—○—), cobalt sulfide from 25 mM (—●—) and 50 mM (—●—) precursor solutions. In the photo two counter electrodes CoS 25 mM (a) and SP Platinum (b). The equivalent circuit (c) used for the fitting of the EIS parameters Rct Rs and Cdl and the Warburg finite diffusion resistance (W).

50 mM and 25 mM solution, in fact the CEs prepared with the 25 mM solution (CoS(25)), see Table 1, have a R_{ct} and R_s lower than those of Pt. However, all R_{ct} values were close to that of Pt.

As can be seen from the fitted parameters shown in Tab. 1, the concentration of the precursor solution is an important parameter with a significant influence in the efficiency of the catalytic EC. In fact, by decreasing the concentration an increase in R_{ct} is observed. The same pattern was observed in the efficiency of the complete DSSCs (Table 2). With 25 mM precursor solution the CEs showed a R_{ct} of 1.31 Ωcm^2 lower than that of Pt. The R_{ct} of the CEs prepared with the 50 mM precursor solution (1.91 Ωcm^2) remained lower than that of Pt but higher than that obtained with the 25 mM solution. The R_{ct} calculated by the EIS for the DSSC (N719 dye) cell was 1.26 Ωcm^2 very close to that obtained with the dummy cells.

Looking at Table 1 we can see that there is a significant decrease of R_s for the CoS(25) counter electrodes, increasing the annealing time from 30 to 120 minutes, however no significant changes have been reported in R_{ct} that remains at around 1.31 Ωcm^2. The catalytic efficiency of the CoS(25) CE has been evaluated also with the redox couple ferrocene/ferrocenium (Fc/Fc^+) using a ferrocene based electrolyte that was prepared following the method proposed by S. Sönmezoğlu et al. [17]. The CoS(25) showed good electrocatalytic performance also with the Fc-based liquid electrolyte, with an R_{ct} value of 2.27 Ωcm^2, further details are available in the supporting informations.

From cyclic voltammetry measurements it was possible to verify the reversibility of the I^-/I_3^- couple redox reaction on the CoS counter electrodes, see Fig. 5. As displayed in Fig 5, the value of the limiting current I_l was the same both in the anodic and in the cathodic part of the voltammogram, and its average is 12.5 mA cm^{-2} for the CoS(25) annealed for 120 minutes. The same electrodes annealed for 60 and 30 minutes have shown slightly lower limiting currents 11.8 and 11.2 mA cm^{-2}, respectively. This limiting current could be further increased, if a narrower gap between electrodes was used. Nevertheless, the I_l value is compatible with the short circuit current of the DSSC shown in Fig. 6.

Table 2
Photo voltaic parameters of DSSCs with different counter electrodes, measured at 1 sun AM1.5 simulated solar light. The CoS(25)A electrode annealed for 240 min.

CE	Dye	Sealing	Area(cm^2)	Jsc(mA cm^{-2})	FF(%)	Voc (mV)	η (%)
Pt	N3	_	1.00	9.05	56.4	702	3.6
CoS(50)	N3	_	1.00	8.48	53.1	703	3.4
CoS(25)	N3	_	1.00	9.23	51.3	700	3.5
CoS(25)A	N3	_	1.00	3.86	23.2	560	0.5
CoS (12,5)	N3	_	1.00	6.08	54.1	701	2.3
CoS(2,5)	N3	_	1.00	4.32	47.9	700	1.4
Pt	N719	Bynel	0.25	13.90	62.4	692	6.0
CoS(25)	N719	Bynel	0.25	14.15	66.7	703	6.6

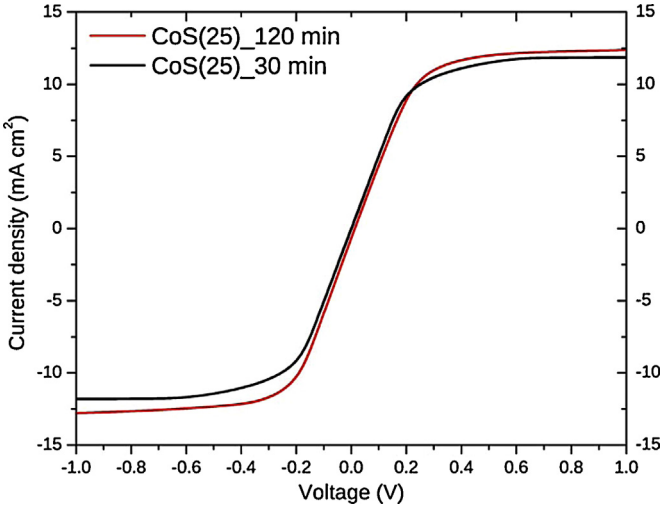

Fig. 5. Voltammogram of HSE in a symmetric device with two CoS(25) counter electrodes, annealed for 120 min(red curve) and 30 min (black curve). The measurement was performed from -1 to 1 V at a scan rate of 10 mVs^{-1}.

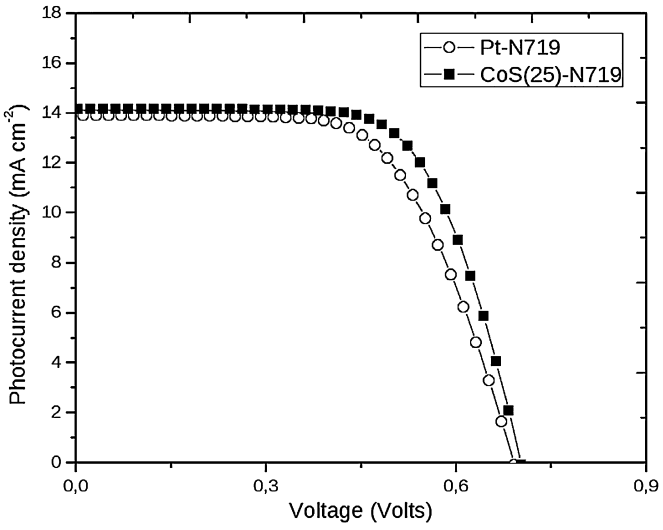

Fig. 6. Current versus voltage curves of 0.25 cm^2 active area DSSCs using N719 and Pt and CoS(25) counter electrodes, 1 sun AM1.5 simulated sun light.

The photovoltaic parameters obtained with different dyes and different CEs prepared from CoS and Pt are presented in Table 2. As can be seen, the performance of the DSSCs follows the same pattern observed for the catalytic activity of the CEs (Table 1). Considering the first batch of samples (1.0 cm^2 active area, N3 dye) we can see that the photocurrent density decreases by decreasing the concentration of the precursor solution. The Jsc of the CoS(25) N3 DSSC was 9.23 $mAcm^2$ and decrease using the CEs prepared from the lower concentration precursor solution (12.5 and 2.5 mM). A lower Jsc was observed using the CoS(50) electrode, in agreement with the pattern observed for Rct in the dummy cells. Notice a slight increase in the fill factor for CoS(50) however for this same cell a small decrease in photocurrent is observed, giving in the end similar efficiencies to CoS(25) cell. The efficiency of the N3 DSSCs was 3.6% using Pt CE and 3.5% using the CoS(25) and decreased by decreasing the concentration of the precursor solution. There is a significant decrease in all of the photovoltaic performance increasing the thermal treatment annealing time from 120 to 240 min (Cos(25)A).

The CEs prepared from the CoS(25) solution were tested in DSSCs with a smaller active area (0.25 cm^2), using a N719 dye and sealed with a Bynel foil, this is our best DSSC configuration. A typical I x V curve under AM1.5 illumination is shown in Fig. 6. For comparison a DSSC with Pt counter electrodes is plotted in the same Figure, the photovoltaic parameters are reported in Table 2. Notice that the solar cell parameters are comparable to those obtained with the Pt CEs. As can be seen, the CoS(25) CE, annealed for 120 minutes, performed slightly better than the platinum counter electrode in terms of cell efficiency (6.6%) and fill factor (66.7%) in the N719 sensitized DSSCs.

The stability of the CoS CEs has been evaluated by subjecting symmetrical cells to electrical stress. As clearly demonstrated in Fig. 7, there is an initial reduction of R_{ct} due to the activation of the electrode, after which R_{ct} tends to increase and stabilizes below 2.0 Ω. R_s undergoes a slight increase as well, yet its value is consistently below 7.0 Ω during the whole test. Regarding the CPE, its value decays from 27 to 25 μFcm^{-2} from the first until the 100th cycle, remaining constant in subsequent cycles. Thus the electrodes showed good stability under electrical stress. It is important to say that with this type of electrical stress the electrodes operate in both reduction and oxidation modes, while in an n-type DSSC cell under normal working conditions under sunlight only the reduction reaction takes place at the counter electrode.

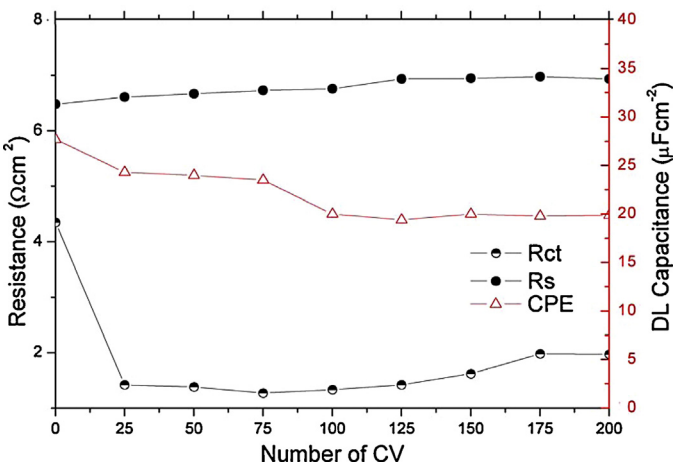

Fig. 7. Stability study of the CoS(25) counter electrode. The electrode is subjected to several cycles of cyclic voltammetry and the Rs, Rct and CPE are monitored. The resistance is shown on the left axis while the capacitance of the double layer is plotted on the right (red).

The transparency of the prepared CoS counter electrodes has been evaluated through the analysis of the transmittance. As can be seen in Fig. 8 the transmittance value for the CoS(25) CE starts at 50% at 700 nm and reach a value of 45% at 400 nm. The screen printed Pt CE has shown a sightly higher transmittance in the whole spectrum. The CoS(50) CE has shown a lower transmittance in comparison with the other samples. Note that the transmittance spectra are from the CE without subtracting the contribution of the FTO, also shown in Fig. 8.

4. Discussion

As presented the proposed counter-electrode preparation method is simple. It requires the deposition of the chemical precursor $Co(DTC)_2$ on the substrate which is completely converted into CoS film by means of a thermal treatment performed at temperatures compatible with those commonly used for DSSC fabrication (350–450 °C). The process for the CEs preparation takes only about 4 h and the electrodes shows transmittances comparable with that of Pt CEs. The chemical precursor used in this work is stable at ambient conditions, cheap

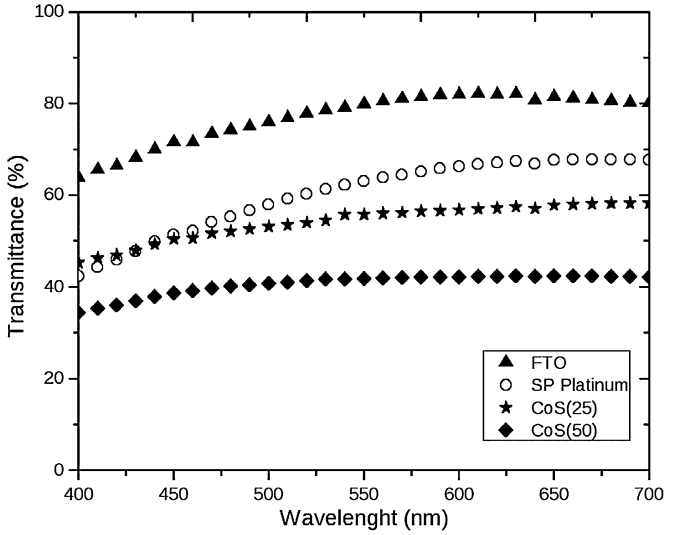

Fig. 8. Transmittance (T%) spectra of the counter electrodes in the visible region (400–700 nm).

and highly soluble in various solvents, some less toxic than chloroform, such as acetone and 1-methyl pyrrolidone. Other chemical precursors with lower degradation temperatures could be considered for this application in order to optimize the characteristics of the final products and to minimize the toxicity of the byproducts.

As can be seen especially from Tables 1 and 2, the concentration of the concentration of the precursor is an important parameter that influences the catalytic activity of the CEs and the photovoltaic performance of the DSSC. As reported the best performances were obtained with the CoS(25) CEs. The pattern observed for the R_{ct} as a function of the concentration of CoDTC, between 2,5 and 25 mM, can be explained in terms of the effective quantity of the catalytic material (CoS) deposited on the surface of the substrate. Using the concentration 2,5 and 12 mM, the electrodes have not shown good catalytic efficiencies in both dummy cells and complete DSSCs devices. The optimal concentration was found to be 25 mM. In fact the CEs prepared using such concentration have shown the best performance both in dummy cells and DSSCs. Note that the concentration of the precursor solution also influence the transparency of the electrodes (Fig. 8). The use of a concentration higher than 25 mM did not lead to any advantage in terms of efficiency nor of transparency of the CEs. In fact the CoS(50) CEs showed a lower transmittance in the visible region than the CoS (25) and their values of R_{ct} and R_s are somewhat higher. The effect of the annealing time was studied between 30 and 120 minutes. As can be see in the XRD patterns shown in Fig. 2, the material is crystalline. The annealing time influences the grain size of the material. The grain sizes calculated from the XRD diffraction spectra showed a significant increase as a function of the annealing time. Looking at Table 1 it can be seen that R_s decreases with increasing processing time. In fact, we can see that the samples processed for 30 minutes have a Rs of 8.57 Ωcm^2, which drops to 7.22 Ωcm^2 for 60 minutes and finally reaches the value of 6.72 Ωcm^2 in the CEs processed for 120 minutes. We attribute the decrease of R_s to the increase of the average grain size. It is important to say that the average grain size has a significant impact on the electronic conductivity in a semiconductor. The increase in the average grain size leads to a decrease in grain boundaries and thus an improvement in the electric conductivity of the bulk material [19]. No significant changes in R_{ct} nor in the capacitance have been observed changing the annealing time. This can be explained looking at the morphology of the films that does not present significant changes varying the annealing time between 30 and 120 minutes as reported in the supporting informations. All of the CoS based CEs were very stable in contact with the HSE electrolyte also in strong electrochemical stressing conditions.

To evaluate the catalytic efficiency of the CE remember that the following reaction (1) occurs at this electrode:

$$I_3^- + 2_e^- \rightarrow 3I^- \quad (1)$$

The rate of this reaction is crucial for the solar cell efficiency and relies on performance of the catalyst deposited on the surface of the cathode. At the cathode a fast recombination of the electrons with the electrolyte is preferable resulting in higher photocurrents and efficiencies. To evaluate the reaction efficiency one can use the Debye response [18]. The Debye response can be represented in form of a circuit, including series resistive components in parallel with a capacitor. For this purpose the Randles circuit can be obtained including a series Warburg element. Such element can be used to calculate the diffusion resistances and the diffusion coefficients [20].

In Fig. 9 there is a 3D representation of the impedance of the dummy cell in three dimensions (Z′,Z″ and ω). In the 3D

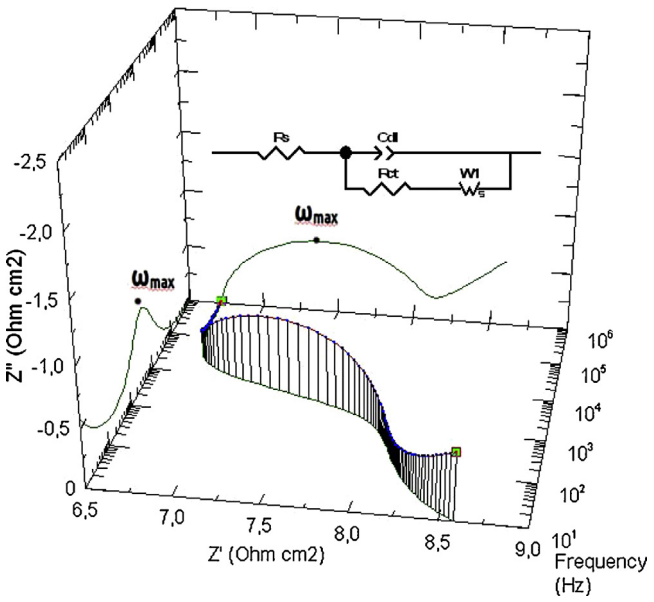

Fig. 9. 3D representation of the EIS spectra of the of the CoS(25) dummy cell. In this graph it is possible to see both the Bode plot (the left projection) and the Nyquist plot. The insert represents the Randles circuit used for the dummy cells fitting in this work.

representation it is possible to see both the value of the R_{ct} (Nyquist plot) and the dependence of the capacitive element in the frequency domain. The value of frequency at the top of the semicircle is ω_{max}. Such frequency is correlated to the time constant (relaxation time), according to the Debye model, that can be written as:

$$\tau = R_{ct} C_{dl} \quad (3)$$

where the term C_{dl} is the capacitance of the double layer at the interface CE\electrolyte and R_{ct} is the charge transfer resistance.

These parameters have been calculated from the curve-fitting to the EIS spectra such as those in Fig. 4. The value of the time constant for the Pt counter electrode is 94.8 μs, comparable with those found in similar studies [20]. The time constants for the CoS counter electrodes, on the other hand, are 32.3 and 45.2 μs for the best electrodes, CoS(25) and CoS(50) respectively. The values of the time constants for CoS(25) and CoS(50) CEs are similar, however

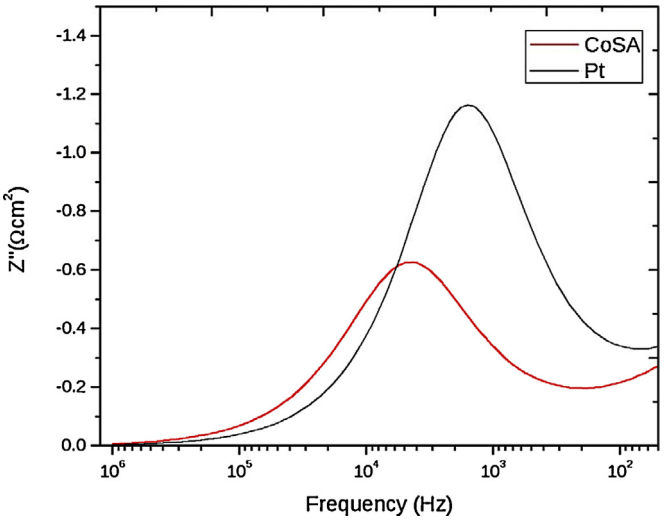

Fig. 10. Bode plots of the CoS(25) (red line) and Pt (black line) of the impedance spectra of the dummy cells.

Table 3
Resume of the main characteristics of other deposition methods published in recent literature.

Material	Method (time-temperature °C)	Rct(Ωcm^2)	Authors (year)	Reference
Co_3S_4	Solvothermal (24h- 150)	0.75	Jie Yang et al. (2014)	[11]
CoS	Potentiodynamic deposition (30 min- 25 °C)	1.43	Jeng-yu Lin (2011)	[22]
CoS	Electrodeposition (30 min–22 °C)	1.80	Mingkui Wang et al. (2009)	[10]
$Co_{8.4}S_8$	Solution processed (30 min - 500)	4.10	Hemar Kumar Mulmudi et al. (2011)	[16]
CoS_2	Chemichal bath deposition (4h- 80)	3.52	Srinivasa Rao *et al.* (2014)	[12]
CoS	Single precursor (30 to 120 min -400)	1.31	M. Congiu et al. (2014)	This work

the electrocatalytic performance of CoS(25) are better due its lower R_{ct}. As can be seen in Table 1, there are not significant differences between the capacitances of the two electrodes and also the exponent n of the CPEs element are equal. It is important to notice that the morphologic characteristics, such as the porosity, the roughness and the active area, can influence the catalytic efficiency of porous counter electrodes [21]. The morphology of the surfaces of CoS(25) and CoS(50) are slightly different and this was confirmed by confocal microscopy (see supporting information). The higher concentration of the precursor solution leads to a surface with a lower number of pores. This can justify the higher R_{ct} (1.91 Ωcm^2) due to the lower number of active sites accessible to the electrolyte. An higher value was observed also for the R_s (9.84 Ωcm^2), probably due to the higher thickness of the film prepared with the more concentrated solution (50 mM), as suggested also by the lower transmittance of the CoS(50) CEs. It is important to remember that, according to the Beer-Lambert law, the intensity of the transmitted light decreases exponentially with the thickness of the material. The time constants calculated from fitting CoS(25) DSSC are slightly higher, 37.9 μs. From the Bode diagrams shown in Fig. 10 we can see that the maximum of the curve relative to the CoS(25) CE is located at a frequency higher than that of the Pt CE. It is important to say that at the frequency corresponding to the maximum of the semicircle (ω_{max}) in the Nyquist plot the following condition is verified in the Debye response:

$$\tau\omega_{max} = 1 \quad (4)$$

The higher is the maximum frequency the lower is the time constant of the system.

The counter electrodes prepared following our method are comparable with those published so far in the recent literature, as can be seen in Table 3. However most of the previous works uses electrodeposition, which involves the use of baths containing high concentrations of Co^{2+} and thiourea, and thus not compatible with the most common techniques used for the large scale production of DSSC modules, such as screen printing and doctor blade processes. On the other hand, the counter electrodes proposed in Ref. [16] and Ref. [12] does not reach R_{ct} lower than that of the conventional Pt counter electrodes.

Our electrodes are very stable in air. A batch of counter electrode was prepared in our laboratory and shipped without special conditions, to the laboratory of C.H.O.S.E (Rome, Italy). After one month from the preparation the counter electrodes were used for the preparation of DSSCs devices and dummy cells. No changes in the cell performance or in the electro catalytic activity were observed.

5. Conclusions

In this work highly stable and efficient CoS based counter electrode from a single chemical precursor were demonstrated for application in DSSCs. The deposited CoS films showed a good adherence to the FTO and a long term stability in ambient conditions. Our electrodes have characteristics close to other CoS based electrodes proposed so far in recent literature, with the advantage of the facility of preparation. The proposed method does not use the toxic components such as thiourea, frequently used in other methods. The chemical precursor used is stable, cheap and can be easily prepared. It is soluble in different solvents and compatible with large scale production techniques, such as ink jet or screen-printing. In addition these electrodes showed in the HSE redox electrolyte a higher electrocatalytic performance than that obtained with the well known platinized. FTO both in dummy cells and in complete DSSCs. As a preliminary result, the CoS counter electrodes have shown a potential application with the ferrocene/ferrocenium redox couple. Such application will be further investigated and optimized in a future study.

Acknowledgements

This work was supported by FAPESP (Fundação de Amparo à Pesquisa do Estado de São Paulo, proc: 2013/07396-7, 13/25028-5, 2013/07296-2 and 2008/57872-1) and CAPES (Coordenação de Aperfeiçoamento de Pessoal de Nível Superior). We want to thank CHOSE (Center for Hybrid and Organic Solar Energy, http://www.chose.uniroma2.it/en/), for having allowed the use of its facilities. A special thanks to Bruna A. Bregadiolli, Dr. Alessandro Lanuti and Silvia L. Fernandes for carrying out part of the measurements.

Appendix A. Supplementary data

Supplementary data associated with this article can be found, in the online version, at http://dx.doi.org/10.1016/j.electacta.2014.11.001.

References

[1] B. O'regan, M. Grfitzeli, A low-cost, high-efficiency solar cell based on dye-sensitized, Nature 353 (1991) 737–740.
[2] S. Mathew, A. Yella, P. Gao, R. Humphry-Baker, C.F.E.N. Ashari-Astani, et al., Dye-sensitized solar cells with 13% efficiency achieved through the molecular engineering of porphyrin sensitizers, Nat. Chem. 6 (2014) 242–247.
[3] G. Khelashvili, S. Behrens, C. Weidenthaler, C. Vetter, A. Hinsch, R. Kern, et al., Catalytic platinum layers for dye solar cells: A comparative study, Thin Solid Films. 511 (2006) 342–348.
[4] B.-K. Koo, D.-Y. Lee, H.-J. Kim, W.-J. Lee, J.-S. Song, H.-J. Kim, Seasoning effect of dye-sensitized solar cells with different counter electrodes, J. Electroceramics 17 (2006) 79–82.
[5] S.A. Yun, Hagfeldt, T. Ma, Pt-free counter electrode for dye-sensitized solar cells with high efficiency, Adv. Mater. (2014), doi:http://dx.doi.org/10.1002/adma.201402056.
[6] H. Wang, Y.H. Hu, Graphene as a counter electrode material for dye-sensitized solar cells, Energy Environ. Sci. 5 (2012)8182, doi:http://dx.doi.org/10.1039/c2ee21905k.
[7] S. AbdulAlmohsin, M. Mohammed, Z. Li, M.A. Thomas, K.Y. Wu, J.B. Cui, Multi-walled carbon nanotubes as a new counter electrode for dye-sensitized solar cells, J. Nanosci. Nanotechnol. 12 (2012) 2374–2379.
[8] B. Park, M. Pazoki, K. Aitola, S. Jeong, E.M.J. Johansson, A. Hagfeldt, et al., Understanding interfacial charge transfer between metallic PEDOT counter electrodes and a cobalt redox shuttle in dye-sensitized solar cells, ACS Appl. Mater. Interfaces 6 (2014)2074–2079, doi:http://dx.doi.org/10.1021/am405108d.
[9] S. Thomas, T.G. Deepak, G.S. Anjusree, T.A. Arun, S.V. Nair, A.S. Nair, A review on counter electrode materials in dye-sensitized solar cells, J. Mater. Chem. A 2 (2014)4474, doi:http://dx.doi.org/10.1039/c3ta13374e.

[10] M. Wang, A.M. Anghel, B. Marsan, N.-L. Cevey Ha, N. Pootrakulchote, S.M. Zakeeruddin, et al., CoS supersedes Pt as efficient electrocatalyst for triiodide reduction in dye-sensitized solar cells, J. Am. Chem. Soc. 131 (2009) 15976–15977.
[11] J. Yang, C. Bao, K. Zhu, T. Yu, F. Li, J. Liu, et al., High catalytic activity and stability of nickel sulfide and cobalt sulfide hierarchical nanospheres on the counter electrodes for dye-sensitized solar cells, Chem. Commun. (2014) .
[12] S. Srinivasa Rao, C.V.V.M. Gopi, S.-K. Kim, M.-K. Son, M.-S. Jeong, A.D. Savariraj, et al., Cobalt sulfide thin film as an efficient counter electrode for dye-sensitized solar cells, Electrochimica Acta (2014), doi:http://dx.doi.org/10.1016/j.electacta.2014.04.010.
[13] S. Ito, P. Chen, P. Comte, M.K. Nazeeruddin, P. Liska, P. Péchy, et al., Fabrication of screen-printing pastes from TiO2 powders for dye-sensitised solar cells, Prog. Photovoltaics Res. Appl. 15 (2007)603–612, doi:http://dx.doi.org/10.1002/pip.768.
[14] P. Gemeiner, M. Mikula, Efficiency of dye sensitized solar cells with various compositions of TiO2 based screen printed photoactive electrodes, Acta Chim. Slovaca 6 (2013)29–34, doi:http://dx.doi.org/10.2478/acs-2013-0006.
[15] I. Jen-La Plante, T.W. Zeid, P. Yang, T. Mokari, Synthesis of metal sulfide nanomaterials via thermal decomposition of single-source precursors, J. Mater. Chem. 20 (2010)6612, doi:http://dx.doi.org/10.1039/c0jm00439a.
[16] H.K. Mulmudi, S.K. Batabyal, M. Rao, R.R. Prabhakar, N. Mathews, Y.M. Lam, et al., Solution processed transition metal sulfides: application as counter electrodes in dye sensitized solar cells (DSCs), Phys. Chem. Chem. Phys. 13 (2011)19307–19309, doi:http://dx.doi.org/10.1039/c1cp22817j.
[17] S. Sönmezoğlu, C. Akyürek, S. Akin, High-efficiency dye-sensitized solar cells using ferrocene-based electrolytes and natural photosensitizers, J. Phys. D. Appl. Phys. 45 (2012)424,101, doi:http://dx.doi.org/10.1088/0022-3727/45/42/425101.
[18] E. Barsoukov, J.R. Macdonald, Impedance Spectroscopy: Theory, Experiment, and Applications, John Wiley & Sons, 2005.
[19] Y. Nishi, R. Doering, Handbook of semiconductor manufacturing technology second edition, CRC Press, 2007, pp. 16–36.
[20] M. a Petrocco, Liberatore, T.M. a Di Carlo, a Reale, Brown, F. Decker, Thermal activation of mass transport and charge transfer at Pt in the I_3^-/I^- electrolyte of a dye-sensitized solar cell, Phys. Chem. Chem. Phys. 12 (2010)10786–10792, doi:http://dx.doi.org/10.1039/c002840a.
[21] J.-Y. Lin, J.-H. Liao, S.-W. Chou, Cathodic electrodeposition of highly porous cobalt sulfide counter electrodes for dye-sensitized solar cells, Electrochim. Acta 56 (2011) 8818–8826. http://dx.doi.org/10.1016/j.electacta.2011.07.080.
[22] J.-Y. Lin, J.-H. Liao, T.-C. Wei, Honeycomb-like CoS counter electrodes for transparent dye-sensitized solar cells, Electrochem. Solid-State Lett. 14 (2011) D41–D44.